

Available online at www.sciencedirect.com

ScienceDirect

journal homepage: www.elsevier.com/locate/ajps

Pharmacokinetics of a ternary conjugate based pH-responsive 10-HCPT prodrug nano-micelle delivery system

Yang Liu ^{a,b,c}, Juan Li ^b, Zhi Li ^b, Xing Tang ^{a,*}, Zhenzhong Zhang ^{b,**}

^a School of Pharmacy, Shenyang Pharmaceutical University, 103 Wenhua Road, Shenyang 110016, China

^b School of Pharmaceutical Sciences, Zhengzhou University, 100 Kexue Avenue, Zhengzhou 450001, China

^c Collaborative Innovation Center of New Drug Research and Safety Evaluation, Henan Province, Zhengzhou 450001, China

ARTICLE INFO

Article history:

Received 30 March 2017

Received in revised form 8 May 2017

Accepted 9 May 2017

Available online

Keywords:

Pharmacokinetics

10-Hydroxycamptothecin

Conjugate

Nano-micelle

PH-responsive

ABSTRACT

A pH-responsive conjugate based 10-hydroxycamptothecin-thiosemicarbazide-polyethylene glycol 2000 (10-HCPT-hydro-PEG) nano-micelles were prepared in our previous study. In the present study, ultra-performance liquid chromatography (UPLC-MS) method is developed to investigate its pharmacokinetics and biodistribution in tumor bearing mice. The results demonstrated that the conjugate circulated for a much longer time in the blood circulation system than commercial 10-HCPT injection, and bioavailability was significantly improved compared with 10-HCPT. *In vivo* biodistribution study showed that the conjugate could enhance the targeting and residence time in tumor site.

© 2017 Production and hosting by Elsevier B.V. on behalf of Shenyang Pharmaceutical University. This is an open access article under the CC BY-NC-ND license (<http://creativecommons.org/licenses/by-nc-nd/4.0/>).

1. Introduction

Multi-drug resistance (MDR) is often the main cause of chemotherapy failure. One reason is that P-glycoprotein (P-gp) on the surface of cancer cells membrane is to discharge small drug molecules [1]. Nano micelles can enter the cell through endocytosis, and due to lack of exocytosis, the concentration of drug in cells can achieve a higher level to improve efficacy [2]. There-

fore, link drug with polymers by chemical bonds to form noneffective conjugate is an ideal design. Which is to release drug by specific mechanism (hydrolysis or enzymatic hydrolysis) to play efficacy after endocytosis, while to normal cells, it remains invalid form and nontoxic [3–7]. Compared with normal cells (pH7.4), tumor cells has acidic microenvironment (pH 5.8–7.2), and lysosome even lower pH value (5.0–5.5). Acid sensitive chemical bond (such as ester bond, oxime key) or chemical structure (e.g. hydrazone, acetal) can

* Corresponding author. Shenyang Pharmaceutical University, No.103, Wenhua Road, Shenyang 110016, China.

E-mail address: tanglab@126.com (X. Tang).

Peer review under responsibility of Shenyang Pharmaceutical University.

** Corresponding author. School of Pharmaceutical Sciences, Zhengzhou University, 100 Kexue Avenue, Zhengzhou 450001, China.

E-mail address: zhenzhongz@126.com (Z. Zhang).

<http://dx.doi.org/10.1016/j.ajps.2017.05.005>

1818-0876/© 2017 Production and hosting by Elsevier B.V. on behalf of Shenyang Pharmaceutical University. This is an open access article under the CC BY-NC-ND license (<http://creativecommons.org/licenses/by-nc-nd/4.0/>).

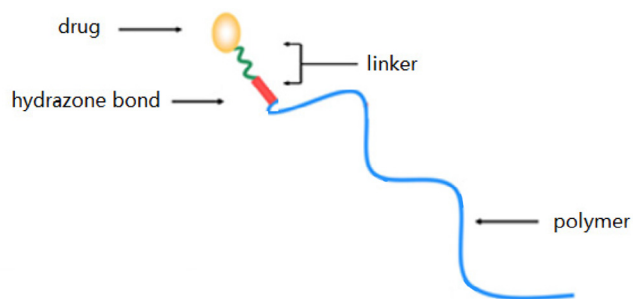


Fig. 1 – Schematic illustration of pH-responsive polymer-drug conjugate.

fracture or change structure through hydrolysis in the acidic environment of the cell, so as to control the release of drugs [8]. In the past decade, pH responsive intelligent drug research become focus in the field of drug delivery [9,10]. Hydrazone bond has been reported in design of pH responsive drug delivery system due to its good stability under the condition of physiological pH and rapid hydrolysis character under acid pH condition [11–14]. (Fig. 1).

10-Hydroxycamptothecin (HCPT) has a broad spectrum of anti-cancer activity *in vitro* and *in vivo* [15]. Its mechanism of therapeutic action is based on targeting nuclear enzyme topoisomerase I (TopoI) by stabilizing a cleavable complex to inhibit DNA S-phase replication and RNA transcription [16]. However, the clinical use of 10-HCPT has been hampered by its poor water solubility and severe side effects, such as myelosuppression and hematuria etc. Combination with a polymer as a prodrug to achieve better targeting and controlled release property is one of the most promising strategies. In our previous study, a water-soluble 10-HCPT-hydro-PEG prodrug was synthesized, as shown in Fig. 2, and it increases the solubility of 10-HCPT by more than 3000 times [17]. The linker contains a pH sensitive hydrazone bond, which breaks in the acidic environment of tumor cell and release drug. The conjugate is amphiphilic and can self-assemble into nano micelle in water. In the current study, we report a validated ultra-performance liquid chromatography (UPLC-MS) assay for the determination of its pharmacokinetics in rats.

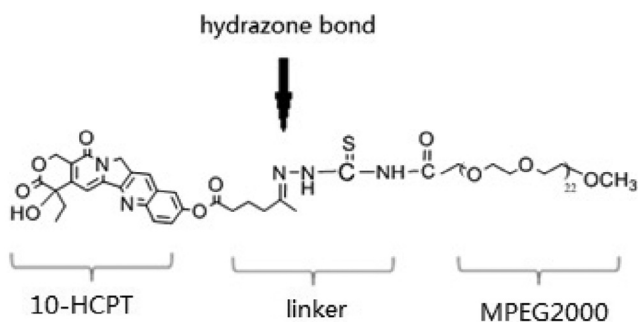


Fig. 2 – Schematic illustration of 10-HCPT-hydro-PEG.

2. Materials and methods

2.1. Materials and animals

2.1.1. Materials

10-HCPT, and EDCI (1-ethyl-3-(3-dimethylaminopropyl)-carbodiimide) were obtained from Sigma Chemical Co. (St Louis, MO, USA). 5-Carbonyl caproic acid and dichloromethane were obtained from Shanghai Topbiochem Ltd. (Shanghai, People's Republic of China). Anhydrous N,N-dimethylformamide (DMF), thiosemicarbazide, and sulfoxide chloride were obtained from Aladdin Industrial Corporation (Shanghai, People's Republic of China). MeO-PEG2000-COOH (molecular weight 2,000 Da) was obtained from Xi'an Ruixi Biological Technology Co. Ltd. (Xi'an, People's Republic of China). Sephadex LH-20 was obtained from Shanghai Yuanye Bio-Technology Co. Ltd. (Shanghai, People's Republic of China). All other chemicals were of analytical grade and were used without further purification.

2.1.2. Animals

All animal research were performed following the protocol approved by the ethics committee of Henan Laboratory Animal Center and followed the guidelines of the Regulations for the administration of affairs concerning experimental animals.

Wistar rats (150~200 g), provided by Henan Academy of Medical Sciences Laboratory Animal Center (qualified number: SCXK-(army), 2007-004).

2.1.3. Statistical analysis

All statistical tests were performed using Statistical Package for Social Science, version 13.0 (SPSS Inc., Chicago, IL, USA). A minimal $P = 0.05$ was used as the significance level for all tests. One-way analysis of variance and Tukey's test were performed on the uptake data. All data are reported as mean \pm standard deviation unless otherwise noted.

2.2. Characterization of conjugate and nano micelles

The conjugate was confirmed by ^1H NMR, ^{13}C NMR, and MALDI-TOF MS. The amphiphilic conjugate could self-assemble into nanosized micelles and the particle size, size distribution, and zeta potential of micelles were determined by dynamic light scattering. The morphology was observed by transmission electron microscopy.

2.3. Stability of nanomicelles *in vitro* and *in plasma*

Hydrazone bond is instable under certain pH conditions, so we test the amount of degradation product (10-carbonyl caproate ester of 10-HCPT) to investigate the stability of nano micelles under different pH conditions. The conjugates were dissolved in a series of PBS solutions (0.01 mol/l) at pH 5.0, 6.0, and 7.4 to give a final concentration of 0.5 mg/ml and were incubated at 37 °C for 48 h. 0.1 ml portions of each solution were withdrawn and centrifuged at 12,000 rpm for 5 min at 0, 0.5, 1, 2, 4, 6, 8, 12, 24, and 48 h and the supernatants were analyzed by UPLC/MS (Agilent Technologies 6460 Triple Quad, Palo Alto, CA, USA; ZORBAX Eclipse XDB-C18 Rapid Resolution HD 2.1 mm \times 100 mm, 1.8 μm , Agilent). Solutions of conjugate

(5.0 mg/ml) and camptothecin with a final concentration of 1.0 $\mu\text{g/ml}$ as an internal standard were added to 5 ml human serum to give a final concentration of 0.5 mg/ml and were incubated at 37 °C. At same time intervals, 100 μl samples were withdrawn. After precipitating the protein with 300 μl acetonitrile, the mixture was vortexed and centrifuged at 12,000 rpm for 5 min. 300 μl of the supernatant was evaporated to dryness under N_2 at 40 °C. The dry extracts were dissolved in 100 μl of acetonitrile for UPLC/MS analysis. The 10-HCPT was then further diluted with human serum to make a set of standards ranging from 0.5 to 1,000 ng/ml and tested quantitatively by the internal standard method. The multiple reactions monitoring mode was used to confirm the precursor ions and select product ions. Full-scan spectra produced a predominant peak of $(\text{MH})^+$ at M/Z 477.0. Collision-induced dissociation of the $(\text{MH})^+$ ion produced a major fragment at M/Z 433.1. Therefore, the transition pair 477.0/433.1 was selected.

2.4. Instrumentation and chromatography conditions

The 10-HCPT in plasma was detected by ultra performance liquid chromatography (UPLC-MS). Chromatographic separation was performed on (Agilent) C_{18} column (1.8 μm , 2.1 mm \times 100 mm). The mobile phase consisted of acetonitrile and 0.01 M NH_4HPO_4 glacial acetic acid/triethylamine (60/40 / 0.7 / 0.3, v / v / v / v, pH to 4.00) with a flow rate of 1.0 ml/min and column temperature of 30 °C; The injection volume was 10 μl . The specific chromatographic conditions were optimized as follows: The multi-reaction monitoring model was used to determine the parent ion and daughter ion. The full scan spectrum produces a main peak at m/z 365.0. The collision induced dissociation fragment is m/z 321.1, thus converting the selection to 365.0/321.1.

2.5. Sample preparation

For the analysis, 150 μl of plasma was mixed with 50 μl of 0.1 N NaOH for 20 min in a water bath at 37 °C, allowing hydrolysis of the conjugate. After this, 0.1 N HCl (50 μl) was added, followed by 20 μl camptothecin (CPT) in acetonitrile (10 $\mu\text{g/ml}$) as internal standard and 600 μl acetonitrile. After vortexing for 2 min, the mixture was sonicated for 5 min and centrifuged at 10,000 rpm for 5 min. The clear supernatant was dried under nitrogen at 40 °C, reconstituted by 100 μl acetonitrile and centrifuged at 12,000 rpm for 10 min before analysis.

2.6. Method validation

Plasma samples were quantified using the ratio of the peak area of 10-HCPT to that of internal standard CPT as the assay response. The peak area ratio (Y) and concentration of 10-HCPT (X) were subjected to a linear regression analysis to calculate the calibration equation and correlation coefficients. Selectivity was assessed by comparing the chromatograms of six different batches of blank rat plasma with the corresponding batch of plasma spiked with 200.0 ng/ml 10-HCPT and 10.0 $\mu\text{g/ml}$ CPT. To evaluate linearity, rat plasma calibration curves were prepared and assayed in triplicate on three consecutive days. The LLOQ was experimentally determined by diluting known concentrations of 10-HCPT in rat

plasma for five replicate determinations. Accuracy and precision were assessed by determining quality control (QC) samples at three concentrations (10.0, 200.0, and 2000.0 ng/ml) on three different validation days. The accuracy was expressed by method recovery and precision by relative standard deviation (RSD). The extraction recoveries of 10-HCPT at three QC levels were determined by comparing the peak area ratios of the analyte to internal standard in the sample that had been spiked with the analyte prior to extraction with samples to which the analyte had been added post-extraction. The internal standard was added to both sets of samples post-extraction. The stability in rat plasma was investigated by placing QC samples under a variety of storage and process conditions. The storage stability under -20 °C freezer conditions was evaluated for 30 days. The freeze-thaw stability was assessed by analyzing QC samples undergoing three freeze-thaw (-20 °C/room temperature) cycles. The stability in the reconstituted solution was investigated by placing QC samples at room temperature for 24 h.

2.7. Pharmacokinetic study

Wistar rats were randomly divided into two groups, each group of six. Group 1: 10-HCPT group; Group 2: 10-HCPT-hydro-PEG group, fasting 12 h before experiment, free drinking water. Rats were administered a single dose of 10-HCPT (5 mg/kg) and 10-HCPT-hydro-PEG (35.1 mg/kg) intravenously. After 10, 20, 30 min, 1, 2, 4, 8, 12, 24, and 48 h of injection, blood samples were collected from the orbital vein, then centrifuged to obtain plasma samples and were stored at -20 °C until analysis. The concentrations of 10-HCPT from plasma were measured using UPLC-MS. Pharmacokinetic data were analyzed using Drug and Statistics (DAS) software version 3.0 (Mathematical Pharmacology Professional Committee of China, Shanghai, People's Republic of China). Using the statistical moment model to process data.

2.8. In vivo biodistribution study

The mice were killed to obtain tissue samples after administration of 10-HCPT (5 mg/kg) and 10-HCPT-hydro-PEG (35.1 mg/kg) intravenously. The organs (heart, liver, spleen, lung, kidney, brain, and tumor) were removed and washed with physiological solution (0.9% NaCl), weighed and stored at -20 °C. Tissues were homogenized in saline. Samples of 200 μl of tissue homogenate were analyzed using the same processing steps as for the plasma samples. The concentrations of 10-HCPT from each tissue homogenate were measured using UPLC/MS. Pharmacokinetic data were analyzed using Drug and Statistics (DAS) software version 3.0 (Mathematical Pharmacology Professional Committee of China, Shanghai, People's Republic of China).

3. Results and discussion

3.1. Characterization of nano micelles

The conjugate was confirmed in our previous study [17]. It can self-assemble into nano micelles. Transmission electron

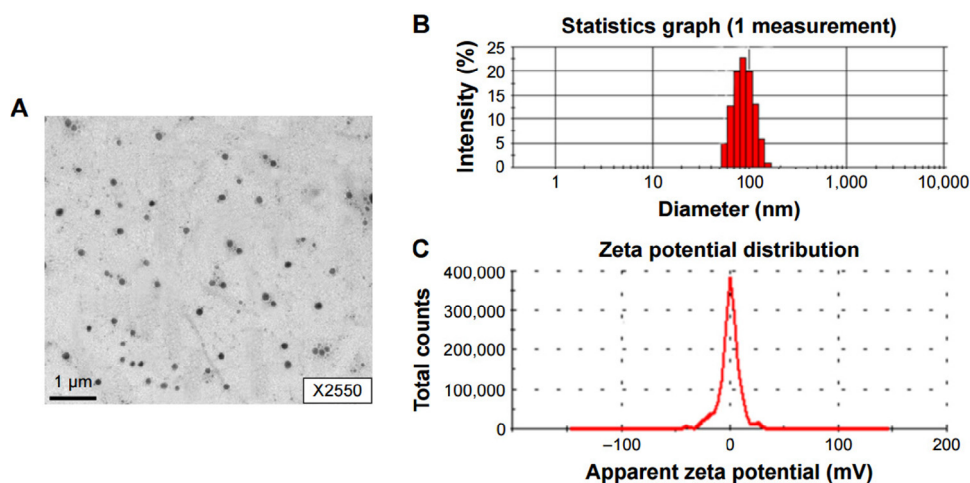


Fig. 3 – TEM image (A), size distribution (B), and zeta potential (C) of nano micelles.

microscopy images revealed their spherical shapes and particle size. The particle size of micelles was 80–100 nm and zeta potential was about -0.23 mV by dynamic light scattering. (Fig. 3).

3.2. Stability of nanomicelles

As shown in Fig. 4, the stability of conjugate was significantly pH-dependent. Specifically, hydrazone bond broke rapidly under pH 6.0, however, in the solution of pH 7.4 and in plasma conjugate contents were 98% and 95% after 4 h, respectively. The contents of conjugate in pH 7.4 PBS or plasma after 48 h were all more than 70%. These results indicate that in blood and at physiological pH levels, the conjugate is relatively stable; however, in the acidic microenvironment of tumor cells, particularly in lysosomes, conjugate breaks quickly.

3.3. Specificity

In the chosen chromatographic conditions, blank rat plasma and plasma samples spiked with 10-HCPT and internal standard after extraction was used for the validation of specificity.

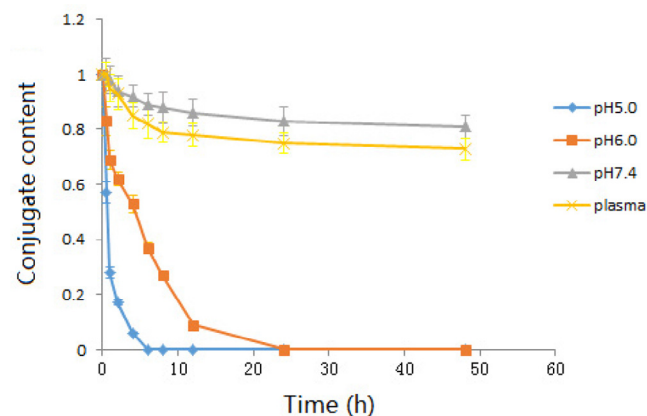


Fig. 4 – Stability of nanomicelles in phosphate-buffered saline and plasma.

The corresponding chromatogram results are shown in Fig. 5. The retention times are 1.599 min and 1.800 min for 10-HCPT and internal standard, respectively. Chromosomes in the main peak, internal standard peaks and adjacent substances can be completely separated between the peaks with a good peaks shape. There were no obvious interfering endogenous substances in rat plasma.

3.4. Calibration curve

10-HCPT concentration in plasma (X) and ratio of CPT internal standard peak area verse 10-HCPT blood drug concentration (Y) was in good linear relationship in the range of 2.0 to 8000.0 ng/ml of 10-HCPT in rat plasma. A typical equation of the calibration curve for rat plasma samples was ($Y = 57.633 X + 13487.17$, $r = 0.9978$, $n = 8$). The lowest concentration (0.2 ng/ml) on the calibration curve was determined as LLOQ.

3.5. Precision

The precision data for intra- and inter day plasma sample are summarized in Table 1. For the assay of 10-HCPT in rat plasma, the intra- and interday precisions ranged from 2.23 to 9.25% and from 4.27 to 10.85%, respectively for three QC levels.

3.6. Recovery

The extraction recovery of 10-HCPT determined at 10.0, 200.0, and 2000.0 ng/mL were 81.83, 83.94 and 87.25%, respectively

Table 1 – Precisions of 10-HCPT in plasma measured by UPLC-MS ($n = 6$).

Concentration (ng/ml)	Concentration measured Intra-day (ng/ml)		Concentration measured Inter-day (ng/ml)	
	Mean \pm SD	RSD (%)	Mean	RSD (%)
10	10.22 \pm 0.945	9.25	10.71 \pm 1.162	10.85
200	206.21 \pm 13.11	6.36	213.85 \pm 18.75	8.77
2000	2032 \pm 45.31	2.23	2086 \pm 89.07	4.27

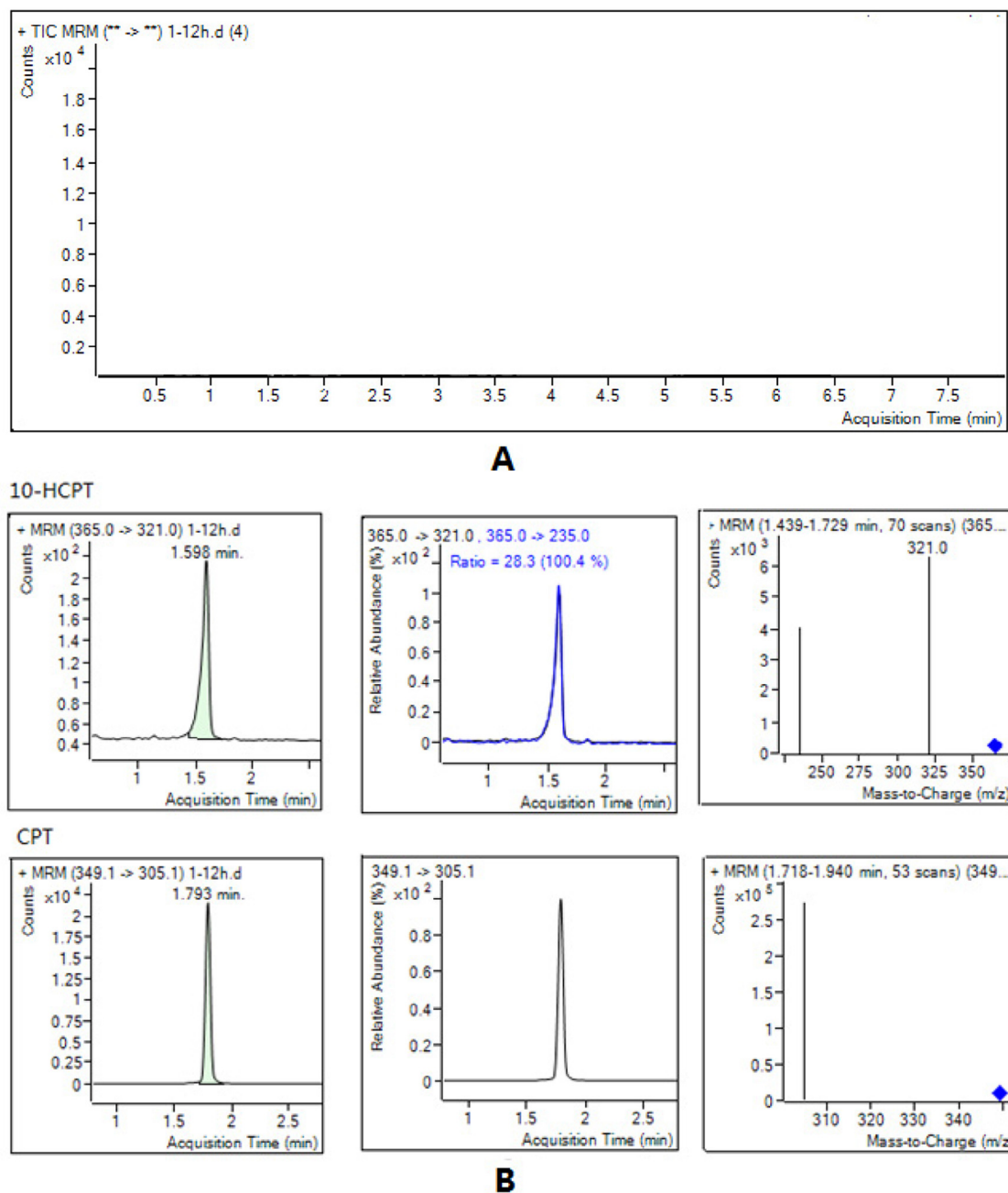


Fig. 5 – UPLC-MS chromatogram of blank plasma sample (A), plasma sample spiked with 10-HCPT, CPT and molecular ion peaks (B).

with % RSD less than 10. ($n = 6$, Table 2). The method recoveries of 10-HCPT in rat plasma, determined at 10.0, 200.00, and 2000.0 ng/mL were 106.71, 100.67, and 97.33%, respectively ($n = 6$, Table 2). The accuracy of the method ranged from 97.33% to 106.71% for three QC levels. The obtained data results meet the FDA guidelines demonstrating the robustness of the validated method developed for analysis of 10-HCPT in plasma [18].

3.7. Stability

Stability was investigated under different conditions such as room temperature, three freeze-thaw cycles and long-term

Table 2 – Recovery of 10-HCPT in plasma measured by UPLC-MS ($n = 6$).

Concentration (ng/ml)	Accuracy (method recovery) (%)		Extraction recovery (%)	
	Mean \pm SD	RSD (%)	Mean \pm SD	RSD (%)
10	106.71 \pm 11.09	10.39	81.83 \pm 2.39	2.92
200	100.67 \pm 3.68	3.66	83.94 \pm 8.74	10.41
2000	97.33 \pm 2.36	2.42	87.25 \pm 4.02	4.61

Table 3 – Stability of 10-HCPT in rat plasma at different conditions (n = 6).

Accuracy (%)	Concentration (ng/ml)		
	10	200	2000
3 Cycles freeze-thaw	97.34 ± 1.26	103.29 ± 2.39	101.83 ± 2.39
Storage (-20 °C, 30 d)	101.88 ± 2.85	98.37 ± 2.39	97.94 ± 2.74
Processed at room temperature	102.12 ± 3.36	103.28 ± 2.39	97.25 ± 3.02

storage (-20 °C, 30 d) for three QC levels. The accuracy results under above conditions indicated that 10-HCPT was stable in rat plasma for at least 30 days when stored at -20 °C and was stable during three freeze-thaw cycles. (Table 3). Processed samples were also stable in the reconstituted solution for at least 24 h at room temperature. The stability was acceptable for pharmacokinetics study.

3.8. Pharmacokinetic study

The mean plasma concentration-time profile in rats after intravenous administration of 5 mg/kg 10-HCPT and 35.1 mg/kg 10-HCPT-hydro-PEG is presented in Fig. 6. The pharmacokinetic parameters were calculated using noncompartmental model. The main pharmacokinetic parameters were presented in Table 4. The plasma concentration of 10-HCPT decreased more rapidly than 10-HCPT-hydro-PEG in the first four hours after injection. The half-life ($t_{1/2}$) of 10-HCPT-hydro-PEG was 10.516 h, which is 5.6 fold higher compared with 10-HCPT, so 10-HCPT-hydro-PEG can significantly delayed the elimination of 10-HCPT in rats. (=h), The $AUC_{(0-\infty)}$ of 10-HCPT-hydro-PEG was 2.06 fold higher compared with 10-HCPT which suggested that 10-HCPT-hydro-PEG could improve the bioavailability of 10-HCPT in rats. The $MRT_{(0-\infty)}$ of 10-HCPT-hydro-PEG (8.975 ± 1.238 h) were significantly longer than those of 10-HCPT (6.146 ± 0.964 h). The results suggested that 10-HCPT-hydro-PEG could circulate for a much longer time in the blood circulation system than 10-HCPT solution, which would result in their higher affinity to tumor cells or extracellular spaces.

Table 4 – Statistical moment model parameters of 10-HCPT in plasma.

Parameters	Unit	10-HCPT (mean ±SD)	10-HCPT-hydro-PEG (mean ±SD)
$AUC_{(0-\infty)}$	μg/l*h	8410.1 ± 3093.6	17341.1 ± 3824.5 ^b
$AUC_{(0-\infty)}$	μg/l*h	8455.8 ± 3101.1	17887.6 ± 4074.6 ^b
$AUMC_{(0-\infty)}$	h*μg/l	53558.5 ± 25164.3	157462.9 ± 46776.7 ^b
$AUMC_{(0-\infty)}$	h*μg/l	56283.9 ± 26021.2	192343.3 ± 64779.8 ^b
$MRT_{(0-\infty)}$	h	6.146 ± 0.964	8.975 ± 1.238 ^a
$MRT_{(0-\infty)}$	h	6.436 ± 1.157	10.561 ± 1.797 ^b
$t_{1/2}$	h	1.859 ± 1.385	10.516 ± 1.158 ^b
T_{max}	h	0.167 ± 0	0.167 ± 0
V	l/kg	26.29 ± 10.304	17.418 ± 2.798 ^b
CL	l/h/kg	2.679 ± 1.068	1.166 ± 0.256 ^a
C_{max}	μg/l	3783.3 ± 1000.4	3967.2 ± 183.4

^a P < 0.05 compared to 10-HCPT injection group.

^b P < 0.01 compared to 10-HCPT injection group.

3.9. In vivo biodistribution assay

The concentrations of 10-HCPT and 10-HCPT-hydro-PEG in heart, liver, spleen, lung, kidney, brain, and tumor were measured after intravenous injection of 10-HCPT solution and 10-HCPT-hydro-PEG nano micelles. The results are presented in Fig. 7. A value of P < 0.05 was considered statistically significant using SPSS. As can be seen, compared with 10-HCPT solution, the $MRT_{(0-\infty)}$ values of conjugate were 4.31-fold in tumors. The $AUC_{(0-\infty)}$ of conjugate in tumor were 7.76-fold higher than those of 10-HCPT solution. The results all suggested that 10-HCPT-hydro-PEG improve the tumor targeting effect of 10-HCPT. The conjugate also exhibited a higher accumulation in the liver, spleen, and lung.

4. Conclusion

A simple, precise, and accurate UPLC-MS method for the quantitation of 10-HCPT in rat plasma with CPT as internal standard was established. The method was successfully applied to a pharmacokinetic study of 10-HCPT-hydro-PEG nano mi-

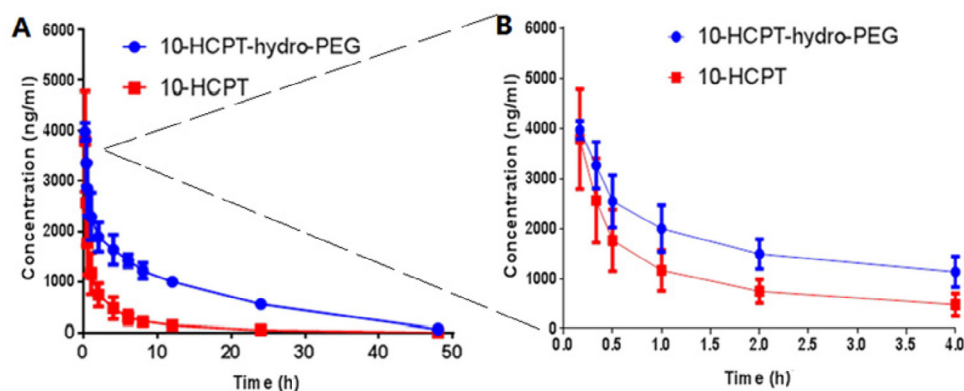


Fig. 6 – Plasma concentration-time curves of 10-HCPT after intravenous administration of 10-HCPT, and 10-HCPT-hydro-PEG at a single dose of 5 mg/kg and 35.1 mg/kg, respectively. The results are presented as the average with standard deviation (mean ± SD, n = 6) A: 10 min~48 h; B: 10 min~4 h.

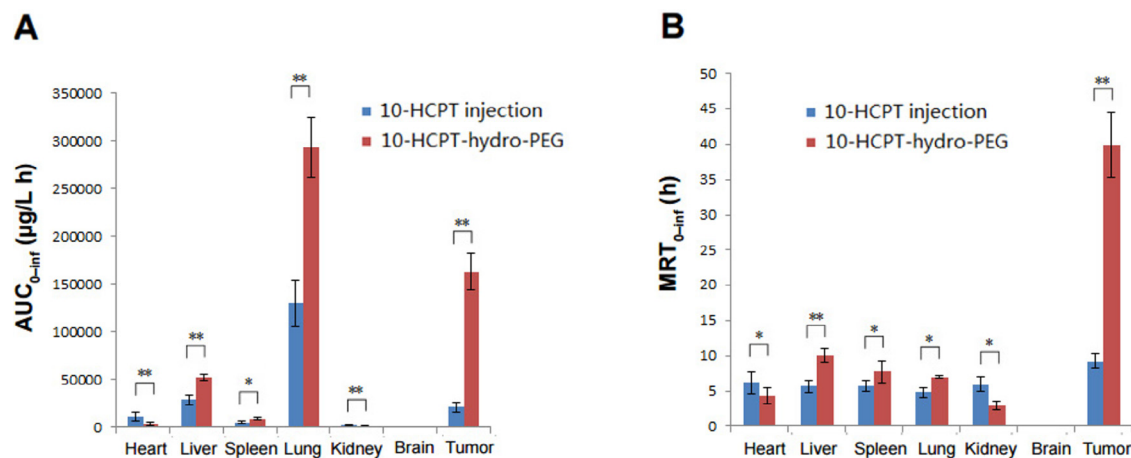


Fig. 7 – In vivo biodistribution of 10-HCPT and 10-HCPT-hydro-PEG to mice (n = 6, A: AUC_{0-inf}; B: MRT_{0-inf}). *P < 0.05 compared to 10-HCPT injection group; **P < 0.01 compared to 10-HCPT injection group. Abbreviations: AUC, area under the curve; MRT, mean residence time.

celles after intravenous administration. In comparison with 10-HCPT solution in plasma, PK study indicated that 10-HCPT-hydro-PEG can prolong the half-life in rats and enhance the targeting and residence time in tumor site. Furthermore, *in vivo* biodistribution study also showed that AUC_(0-inf) values of nano micelles in tumor were significantly higher than those for 10-HCPT injection. These results suggest that nano micelle can be considered as a promising targeted delivery system to improve therapeutic efficacy.

Acknowledgments

This work was supported by the Major National Scientific Research Projects (2015CB932103).

REFERENCES

- [1] Friberg S, Nyström AM. NANOMEDICINE: will it offer possibilities to overcome multiple drug resistance in cancer? *J Nanobiotechnology* 2016;14(1):17.
- [2] Karthikeyan R, Koushik OS. Nano drug delivery systems to overcome cancer drug resistance – a review. *J Nanomed Nanotechnol* 2016;7(3):1–9.
- [3] Bao Y, Yin M, Hu X, et al. A safe, simple and efficient doxorubicin prodrug hybrid micelle for overcoming tumor multidrug resistance and targeting. *J Control Release* 2016;235:182–194.
- [4] Sheng Y, You Y, Chen Y. Dual-targeting hybrid peptide-conjugated doxorubicin for drug resistance reversal in breast cancer. *Int J Pharm* 2016;512(1):1–13.
- [5] Bala V, Rao S, Boyd BJ, et al. Prodrug and nanomedicine approaches for the delivery of the camptothecin analogue SN38. *J Control Release* 2013;172:48–61.
- [6] Guo X, Shi C, Wang J, et al. PH-triggered intracellular release from actively targeting polymer micelles. *Biomaterials* 2013;34(34):4544–4554.
- [7] Chen Y, Zhang W, Huang Y, et al. Pluronic-based functional polymeric mixed micelles for co-delivery of doxorubicin and paclitaxel to multidrug resistant tumor. *Int J Pharm* 2015;488:44–58.
- [8] Pang X, Jiang Y, Xiao Q, et al. PH-responsive polymer-drug conjugates: design and progress. *J Control Release* 2016;222:116–129.
- [9] Moku G, Gulla SK, Nimmu NV. Delivering anti-cancer drugs with endosomal pH-sensitive anti-cancer liposomes. *Biomater Sci* 2016;4(4):627.
- [10] Koyamatsu Y, Hirano T, Kakizawa Y, et al. PH-responsive release of proteins from biocompatible and biodegradable reverse polymer micelles. *J Control Release* 2014;173(1):89–95.
- [11] Ma Y, Fan X, Li L, et al. PH-sensitive polymeric micelles formed by doxorubicin conjugated prodrugs for co-delivery of doxorubicin and paclitaxel. *Carbohydr Polym* 2016;137:19–29.
- [12] Yina Y, Fub C, Lia M, et al. A pH-sensitive hyaluronic acid prodrug modified with lactoferrin for glioma dual-targeted treatment. *Mater Sci Eng C Mater Biol Appl* 2016;67:159–169.
- [13] Liu N, Li B, Gong C, et al. A pH- and thermo-responsive poly(amino acid)-based drug delivery system. *Colloids Surf B Biointerfaces* 2015;136:562–569.
- [14] He Q, Gao Y, Zhang L, et al. A pH-responsive mesoporous silica nanoparticles-based multi-drug delivery system for overcoming multidrug resistance. *Biomaterials* 2011;32(30):7711–7720.
- [15] Chen Q, Pan G, Xiong L, et al. Characterization and quantification of 10-hydroxycamptothecin in *Camptotheca acuminata* and its medicinal preparation by liquid chromatography-ion trap mass spectrometry. *Biomol Chromatogr* 2013;27:1615–1620.
- [16] Ni Y, Wang Y, Kokot S. Study of the interaction between 10-hydroxycamptothecin and DNA with the use of ethidium bromide dye as a fluorescence probe. *Sens Actuators B Chem* 2011;156(1):290–297.
- [17] Liu Y, Li D, Guo X, et al. A pH-responsive prodrug delivery system of 10-HCPT for controlled release and tumor targeting. *Int J Nanomedicine* 2017;12:2227–2242.
- [18] USDHHS, FDA, CDER. Guidance for industry: bioanalytical method validation, U.S. Department of Health and Human Services, Food and Drug Administration, Center for Drug Evaluation and Research (CDER), Center for Veterinary Medicine (CV); 2013. Available from: <https://www.fda.gov/downloads/Drugs/Guidances/ucm368107.pdf>. [Accessed September 2013].